Coherent Dynamics of the Localized Vibrational Modes of Hydrogen in CaF_2

Jon-Paul R. Wells,[1,2,*] Chris W. Rella,[3,†] Ian V. Bradley,[1,2] Ian Galbraith,[1] and Carl R. Pidgeon[1]

[1]*Department of Physics, Heriot-Watt University, Edinburgh EH14 4AS, United Kingdom*
[2]*FELIX Free Electron Laser Facility, FOM–Institute for Plasmaphysics "Rijnhuizen," P.O. Box 1207, 3430 Be Nieuwegein, The Netherlands*
[3]*FOM–Institute for Atomic and Molecular Physics, Kruislaan 407, 1098 SJ Amsterdam, The Netherlands*
(Received 18 November 1999)

We report the observation of giant quantum coherence effects in the localized modes of ionized hydrogen in synthetic fluorite. Infrared free induction decay experiments on the substitutional H^- center show dramatic modulations at negative delay times due to interference between multiple vibrational levels. Spectrally resolving the degenerate four wave mixing signal allows unambiguous assignments of the participating vibrational states. The dependence of the signal intensity upon the delay path between the exciting free electron laser pulses can be accounted for in terms of the resonant third order polarization with a common dephasing time for the excited states.

PACS numbers: 78.30.Hv, 41.60.Cr, 42.50.Md, 63.20.Pw

Nonradiative relaxation processes can be extremely important for the deexcitation of molecular impurities in crystals, glasses, and liquids. A classic example is tetrahedrally coordinated V^{3+} which in many oxide compounds (e.g., $LiAlO_2$ [1]) exhibits radiative quantum efficiencies down to less than 1%. As such, nonradiative relaxation represents a serious limitation to the development of room temperature solid state lasers operating in the near- and midinfrared regions. Recent studies on isoelectronic Cr^{4+} doped into Mg_2SiO_4 crystals have shown the importance of local modes in mediating nonradiative energy transfer to the lattice band phonon states [2]. Studies of the relaxation of SH vibrational stretch modes in amorphous As_2S_3 have also shown the importance of local modes when accounting for the relaxation of diatomic molecules in solids [3].

Despite the central role which localized vibrational modes are known to play in nonradiative decay processes, comparatively little is known about their time evolution during the optical pumping cycle. The earliest studies involve the use of CO_2 lasers to perform saturation measurements for H^- in CaF_2. In 1971, Lee and Faust [4] demonstrated saturation of the H^- local mode absorption, while the study of Lang *et al.* [5] measured a 10 K lifetime of 17 ps and tracked its temperature dependence up to 110 K. The residual (10 K) lifetime and its behavior with respect to temperature were attributed to three-phonon anharmonic decay. At the time of writing, only one time-resolved study utilizing pulses shorter than the H^- local mode lifetime [6] has involved the direct excitation of localized modes, as this has been beyond experimental capability until the advent of the free electron laser and more recently, mid-IR optical parametric amplifiers. Indeed, no coherent investigations have been performed to the knowledge of the authors. In this Letter we have applied a new technique, the spectrally resolved infrared free induction decay (IR FID), to characterize the coherent dynamics of the H^- substitutional localized vibrational mode in CaF_2. Together with the time-integrated two-pulse IR FID, this technique can be used to detect and characterize the excited state vibrational populations. These methods provide a way of transferring population in a controlled fashion and determining the dephasing rates of the excited states involved.

Localized vibrational modes are created when a light defect is introduced to a crystalline lattice if the force constants between the impurity and its neighbors are similar to those between pairs of neighboring host lattice ions [7]. For H^- ions diffused into CaF_2 crystals, the hydrogen ions occupy a substitutional position and thus reside in a center with tetrahedral point group symmetry [8]. To a very good approximation, the localized modes can be considered to be vibrations of the hydrogen alone with the rest of the lattice, composed of much heavier ions, remaining stationary. The fundamental vibration $[\Gamma_1(\nu = 0) \rightarrow \Gamma_5(\nu = 1)]$ of this defect is triply degenerate, has a frequency of 965.2 cm^{-1}, and a population decay time T_1 of 45 ps (this value is obtained from Ref. [6] and has been independently confirmed by the authors at FELIX).

These experiments were performed at the Dutch Free Electron Laser in Nieuwegein (FELIX) which was tuned to the fundamental resonance of the substitutional H^- local mode in CaF_2 single crystals. The output of FELIX was split into two pulses by an 85% transmitting ZnSe beam splitter and then both focused onto the sample with a 12.5 cm off-axis parabolic mirror. In these experiments, performed in a non-co-linear degenerate four wave mixing (DFWM) geometry, the first pulse with wave vector $\mathbf{k}_1$ creates a coherent polarization in the medium, and the second pulse with wave vector $\mathbf{k}_2$ arrives at the sample after a delay time τ. If τ is smaller than the dephasing time of the polarization, an interference grating is produced from which $\mathbf{k}_2$ can be self-diffracted along the phase matched direction $|2\mathbf{k}_2 - \mathbf{k}_1|$. The diffracted energy is then measured as a function of delay τ. The IR-FID technique is related to the recent vibrational echo [9] experiments first performed on the CO stretch mode of tungsten hexacarboyl

 0031-9007/00/84(21)/4998(4)$15.00

in glassy dibutylphalate. However, in the vibrational echo, the second pulse reverses the phase evolution of the different frequency components of an inhomogeneously broadened vibrational line leading to a superradiant burst (or echo). The IR FID is in fact a vibrational echo performed on a homogeneously broadened line.

The Fig. 1(*a*) curve shows the IR-FID signal recorded for a sample temperature of 10 K. In this measurement, powers of less than 80 nJ per pulse were used with a FELIX spectral width of 4 cm^{-1}. The signal observed is associated with the free induction decay of the $\Gamma_1(\nu = 0) \rightarrow \Gamma_5(\nu = 1)$ transition alone, as the spectral width of FELIX is not sufficient to exceed the vibrational anharmonicity. Figure 1(*b*) curve shows the vibrational signal recorded under the same conditions, except that the laser bandwidth has been broadened to 45 cm^{-1} and the power increased to over 1.5 μJ per pulse. The transient is striking in that large modulations are present in the *negative time* signal. These modulations arise because the FELIX linewidth significantly exceeds the anharmonicity of the system, allowing large numbers of vibrational quanta to undergo excited state absorption transitions.

Additional information can be extracted from the IR FID by dispersing the signal into its constituent frequencies in a monochromator for a given (fixed) delay time and excitation frequency. In this fashion, one may *spectrally resolve* the IR-FID signal. Figure 1(d) shows the spectrally resolved IR FID for a +4 ps delay between pump and probe. As can be seen there are three frequencies contributing to the signal 954 ± 2, 965 ± 2, and 978 ± 2 cm^{-1}. These correspond to the fundamental vibration $[\Gamma_1(\nu = 0) \rightarrow \Gamma_5(\nu = 1)]$ and two excited state absorption transitions, $\Gamma_5(\nu = 1) \rightarrow \Gamma_3(\nu = 2)$ at 978 cm^{-1} and $\Gamma_5(\nu = 1) \rightarrow \Gamma_5(\nu = 2)$ at 954 cm^{-1}. In fact, if one increases the gain sufficiently even the $\Gamma_5(\nu = 1) \rightarrow \Gamma_1(\nu = 2)$ resonance at 928 ± 3 cm^{-1} can be observed in the spectrally resolved IR FID, and thus all three $\nu = 2$ states of the anharmonic oscillator are seen to contribute to the coherently excited vibrational ensemble. Thus the spectrally resolved IR FID provides a powerful new method of experimentally extracting the vibrational states participating in the stepwise excitation of an anharmonic ladder system.

To fully and quantitatively understand the origin of the dramatic beats recorded at negative time delay we must look for the resonant third order polarization in the $|2\mathbf{k}_2 - \mathbf{k}_1|$ direction. A calculation of this can be done using perturbation theory for the density operator [10]. The expectation value of the third order polarization can be written as

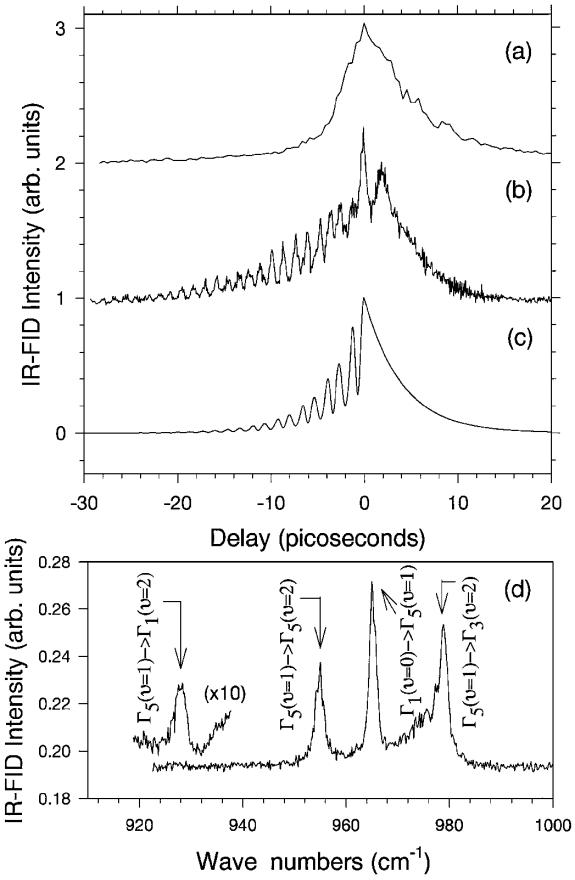

FIG. 1. 10 K IR-FID signal for resonantly exciting the 965.2 cm^{-1} $\Gamma_1(\nu = 0) \rightarrow (\nu = 1)$ fundamental vibration. Employing [curve (*a*)] a power of 80 nJ per pulse and FELIX spectral width 4 cm^{-1}, and [curve (*b*)] a power of 1.5 μJ per pulse and 45 cm^{-1} FELIX spectral width. (*c*) The model fit to (*b*) according to Eqs. (2) and (3). (d) Spectrally resolved IR FID exciting the fundamental vibration with a fixed positive time delay of nearly 4 ps. The vibrational states are labeled by the appropriate irreducible representation (Γ_i) under the tetrahedral point group (T_d).

$$\langle \mathcal{P}^3(t) \rangle \propto \int_{t_0}^{t} \int_{t_0}^{t_1} \int_{t_0}^{t_2} e^{\gamma(t_3 - t)} E(t_1) E(t_2) E(t_3) \, \mathrm{Tr}\{\mathcal{P}_I(t) [\mathcal{P}_I(t_1), [\mathcal{P}_I(t_2), [\mathcal{P}_I(t_3), \rho_0]]]\} \, dt_3 dt_2 dt_1 \,, \tag{1}$$

where $E(t)$ is the electric field of the pulses, $\mathcal{P}_I(t)$ is the polarization operator in the interaction picture, and ρ_0 is the ground state density operator. We have included a single dephasing rate γ in the model which describes the dephasing of any induced polarization. The product of the three electric fields gives rise to many components propagating in discrete directions. From these we select only that which propagates in the $|2\mathbf{k}_2 - \mathbf{k}_1|$ direction with its associated temporal oscillation. Using this, expanding the commutators in Eq. (1), and evaluating the trace with the aid of the completeness relation, one can select out the resonant terms. For the energy level scheme, five terms remain as depicted in Fig. 2. The solid arrows indicate the transitions induced by the incoming photons, while the dashed arrows

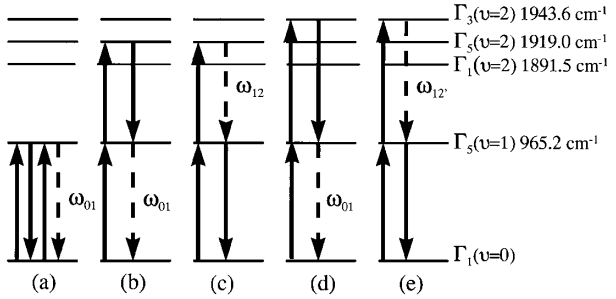

FIG. 2. Schematic diagram of the lower vibrational states of the T_d center in CaF_2:H^- and resonant contributions to the DFWM signal.

indicate the oscillating polarization which is reradiated in the signal direction after the second pulse arrives. Figure 2(a) involves only the fundamental transition and contributes only at positive time delays. Figures 2(b)–2(e) involve two of the excited levels of the ($\nu = 2$) triplet and contribute strongly at both negative and positive time delays. There are several other terms which contribute only at precisely zero delay which give rise to the so-called coherent artifact spike which we can ignore as it gives no new information regarding the vibrational dynamics.

As the FELIX pulses are much shorter than the observed decays we can approximate their shapes as δ functions. This allows us to analytically evaluate the time-integrated four wave mixing signal $S(\tau)$ as

$$S(\tau > 0) \propto \frac{\mu_{01}^4 e^{-2\gamma\tau}}{2\gamma}\left[4\mu_{01}^4 + \mu_{12}^4 + \mu_{12'}^4 + \frac{8\mu_{12}^2\mu_{12'}^2\gamma^2}{4\gamma^2 + (\Delta_{12} - \Delta_{12'})^2} - \frac{16\mu_{01}^2\mu_{12}^2\gamma^2}{4\gamma^2 + \Delta_{12}^2} - \frac{16\mu_{01}^2\mu_{12'}^2\gamma^2}{4\gamma^2 + \Delta_{12'}^2}\right], \quad (2)$$

$$\begin{aligned} S(\tau < 0) \propto \frac{\mu_{01}^4 e^{2\gamma\tau}}{\gamma}\Bigg[& \mu_{12}^4 + \mu_{12'}^4 + \mu_{12}^2\mu_{12'}^2\cos[(\Delta_{12} - \Delta_{12'})\tau] \\ & - 2\mu_{12}^4\frac{2\gamma^2\cos(\Delta_{12}\tau) + \gamma\Delta_{12}\sin(\Delta_{12}\tau)}{4\gamma^2 + \Delta_{12}^2} - 2\mu_{12'}^4\frac{2\gamma^2\cos(\Delta_{12'}\tau) + \gamma\Delta_{12'}\sin(\Delta_{12'}\tau)}{4\gamma^2 + \Delta_{12'}^2} \\ & + 2\mu_{12}^2\mu_{12'}^2\frac{2\gamma^2\cos[2(\Delta_{12} - \Delta_{12'})\tau] + \gamma(\Delta_{12} - \Delta_{12'})\sin[2(\Delta_{12} - \Delta_{12'})\tau]}{4\gamma^2 + (\Delta_{12} - \Delta_{12'})^2} \\ & - 2\mu_{12}^2\mu_{12'}^2\frac{2\gamma^2\cos[(2\Delta_{12} - \Delta_{12'})\tau] + \gamma\Delta_{12}\sin[(2\Delta_{12} - \Delta_{12'})\tau]}{4\gamma^2 + \Delta_{12}^2} \\ & - 2\mu_{12}^2\mu_{12'}^2\frac{2\gamma^2\cos[(2\Delta_{12'} - \Delta_{12})\tau] + \gamma\Delta_{12'}\sin[(2\Delta_{12'} - \Delta_{12})\tau]}{4\gamma^2 + \Delta_{12'}^2}\Bigg], \end{aligned} \quad (3)$$

where Δ_{12} is the detuning of the optical frequency from the $\Gamma_5(\nu = 1) \rightarrow \Gamma_5(\nu = 2)$ transition energy, and similarly $\Delta_{12'}$ is the optical detuning of the $\Gamma_5(\nu = 1) \rightarrow \Gamma_3(\nu = 2)$ transition.

The dominant terms for negative time delays are the first three terms in Eq. (3) which show the exponential growth and an oscillation at the difference frequency between two of the excited states of the $\nu = 2$ triplet. Diagrammatically this term arises from the interference between diagrams Figs. 2(c) and 2(e). The incoming $\mathbf{k}_2$ pulse generates polarizations oscillating at ω_{12} and $\omega_{12'}$ which evolve independently for time τ before the emission in $|2\mathbf{k}_2 - \mathbf{k}_1|$ occurs. The interference of these two polarizations is the origin of the strong beats at negative time delays. Superimposed on these beats is a modulation on a longer time scale of around 10 ps.

Figure 1(*c*) shows the model fit to the data of Fig. 1(*b*) using the equations derived above [Eqs. (2) and (3)]. The fit was obtained by adjusting the dephasing rate γ to fit the positive delay signal, giving $T_2 = 8.0 \pm 0.5$ ps. This value corresponding closely to the linewidth of the spectrally resolved IR FID however, is nearly half that inferred from the absorption line profile (of 16.3 ps) due to a power broadening of the linewidth. Only at the very lowest powers used is the IR-FID linewidth comparable to that measured using the absorption line profile. The combinations of these T_2 measurements are eminently sensible in the light of the 45 ps lifetime measured in Ref. [6]. The feature at positive delay [curve (*b*) of Fig. 1] is not explained but may be associated with higher order coherences not included in the present model. We have extended our model to include the influence of inhomogeneous broadening and find that although oscillations at positive delays are possible, they never coexist with beats at negative times. The $\nu = 2$ excited state splittings were held constant at the values inferred by Raman scattering experiments [11]. This fit gives qualitative agreement with experiment despite the exclusion of terms arising from higher order coherences. Thus this simple model of the third order polarization propagating in the signal direction can qualitatively account for the observed IR-FID signals, a fact which bodes well for

attempts to tackle more complicated, perhaps less well-characterized systems.

In conclusion, we have demonstrated anharmonic ladder climbing and isolated the vibrational states participating via spectrally resolved infrared free induction decay experiments for CaF_2:H^- substitutional localized modes of vibration. This anharmonic ladder climbing can be manipulated by altering the laser parameters such as pulse length and frequency of excitation. For resonant excitation of the fundamental vibrational frequency, dramatic oscillations have been observed on the IR-FID transients at negative time delays because of interference between multiple coherently excited vibrational states. The observed coherent transients are quantitatively described in terms of a simple model of the third order polarization of the H^- oscillators, and a good account is obtained for a four-level excitation scheme.

This work was supported by the EPSRC (through research Contract No. GR/M/22374) and FOM. We appreciate the skillful assistance of the FELIX staff, in particular, Dr. A. F. G. van der Meer. In addition, the authors would like to thank Dr. Glynn D. Jones of the University of Canterbury, New Zealand, for supplying the hydrogenated samples.

*Author to whom correspondence should be addressed. Email address: wells@rijnh.nl

†Current address: Stanford Picosecond FEL Center, W. W. Hansen Laboratory, Stanford University, Stanford, CA 94305-4085.

[1] S. Kueck and P. Jander, Chem. Phys. Lett. **300**, 189 (1999).
[2] D. M. Calistru, S. G. Demos, and R. R. Alfano, Phys. Rev. Lett. **78**, 374 (1997).
[3] J. R. Engholm, C. W. Rella, H. A. Schwettman, and U. Happek, Phys. Rev. Lett. **77**, 1302 (1996).
[4] L. C. Lee and W. L. Faust, Phys. Rev. Lett. **26**, 648 (1971).
[5] P. T. Lang, W. J. Knott, U. Werling, K. F. Renk, J. A. Campbell, and G. D. Jones, Phys. Rev. B **44**, 6780 (1991).
[6] C. P. Davison, J. A. Campbell, J. R. Engholm, H. A. Schwettman, and U. Happek, J. Lumin. **76&77**, 628 (1998).
[7] R. C. Newman, in *Infrared Studies of Crystal Defects*, edited by B. R. Coles and Sir Nevil Mott, Monographs on Physics (Taylor & Francis, London, 1973).
[8] R. J. Elliott, W. Hayes, G. D. Jones, H. F. Macdonald, and C. T. Sennett, Proc. R. Soc. London A **289**, 1 (1965).
[9] A. Tokmakoff, A. S. Kwok, R. S. Urdahl, R. S. Francis, and M. D. Fayer, Chem. Phys. Lett. **234**, 289 (1995).
[10] W. H. Louisell, *Quantum Statistical Properties of Radiation* (Wiley, New York, 1973).
[11] C. A. Freeth, J. Phys. Condens. Matter **1**, 9077 (1989).